Iranian Journal of Materials Science and Engineering, Vol. 21, Number 1, March 2024
RESEARCH PAPER

Electro-Optical Properties of CdS Thin Films by Chemical Bath Technique

S. H. Mane

samratmane95@gmail.com

Department of Physics, Datar, Behere and Joshi College, Chiplun, Dist- Ratnagiri, India.415605

Received: December 2023 **Revised: March 2024** **Accepted: March 2024**
DOI: 10.22068/ijmse.3530

Abstract: *In this research work, a Cadmium Sulphide thin film was deposited onto a glass substrate in a non-aqueous medium at 80°C. The various physical preparative parameters and the deposition conditions, such as the deposition time and temperature, concentrations of the chemical species, pH, speed of mechanical stirring, etc., were optimized to yield good quality films. The as-prepared sample is tightly adherent to the substrate's support, less smooth, diffusely reflecting and was analyzed for composition. The synthesized film is characterized using X-ray diffraction (XRD), electrical, and optical properties. It appears that the composites are rich in Cd. The grown CdS thin film had an orange-red color. A band gap of CdS thin film is 2.41 eV. The average crystallite size of the CdS film was 21.50 nm. The resistivity of the CdS thin film is about 5.212 x 10^5 Ωcm.*

Keywords: *CdS thin film, Low cost, CBD techniques, Electrical and optical properties.*

1. INTRODUCTION

The most important factor influencing the electro-optical characteristics of semiconducting materials is doping. There are situations when the measured carrier concentration is larger than what would be predicted from the dopant contribution alone after the doping impurities are added. This indicates that carrier manufacturing is caused by the stoichiometric disorder [1, 2, 3]. However, in certain instances, the carrier concentration consistently falls short of the anticipated levels. The carrier transport mechanism across the grain borders is impacted by the segregation of these inactive dopant atoms along the grain boundaries [1, 3, 4]. It is crucial to undertake research on electrical conduction and comprehend the conduction mechanism behind CdS thin film formation. Consequently, these investigations were conducted in two phases: Thus, these investigations were divided into two sections: the thermoelectric power and electrical conductivity examinations.

2. EXPERIMENTAL PROCEDURES

2.1. Materials

Analytical grade cadmium sulphate, thiourea, liquid ammonia and triethanolamine were used as precursor chemicals. Stoichiometric volumes of cadmium sulphate and thiourea were added to a reaction bath in proportion to each other and allowed to react in an alkaline medium to prepare CdS thin films.

2.2. Deposition of the Samples

The CdS thin films were deposited on the glass substrates using the liquid phase chemical bath deposition (LPBCD) method developed by us /7, 12, 13, 17/. For the deposition, 10 ml (1 M) cadmium sulphate solution was added to a 250 ml glass vessel. Triethanolamine (TEA) and liquid ammonia were added dropwise to increase the pH of the reacting solution and improve the adhesion of the film to the substrate surface. To this end, 10 ml (1 M) of thiourea was added. The pH of the final reaction mixture was 11. For each of the materials in this series, the film stoichiometry was maintained by adjusting the ion concentration volumes of the cadmium sulphate. The total volume of the reaction bath was brought to 200 ml by adding double distilled water. The reaction vessel was then transferred to a constant temperature oil bath whose temperature was maintained at 58°C. The thoroughly cleaned glass substrates of appropriate dimensions were mounted on a specially designed substrate holder and connected to a constant speed motor that rotated them at 70±2 rpm. The deposition was continued for 90 minutes, then the samples were removed from the reaction bath and detached from the substrate holder, washed with double distilled water, dried and then stored in a dark desiccator.

2.3. Characterization of the Samples

The resulting composite film was then characterized based on its composition, structure,

[DOI: 10.22068/ijmse.3530]

and optical properties to determine the effects of the deposition parameters. The X-ray diffraction method was used to study the structure of the deposited sample. For this purpose, an X-ray diffractometer Philips PW-1710 with CuKα line (λ=1.5406A°) in the 2θ range from 200 to 800 was used. The diffractogram was further analyzed to determine the crystal dimensions and hence the structure. The optical constants such as the absorption coefficient (α) and the optical gap (E_g), as well as the nature of the transitions for this film, were determined based on the measurement of the optical absorption spectra. For this purpose, a Shimadzu UV-3600 spectrophotometer was used, varying the incident wavelength from 500 nm to 1300 nm. The optical absorption was recorded stepwise for each of the wavelengths.

3. RESULTS AND DISCUSSION

3.1. Optical Studies

Here, the optical absorption spectra in the 500–1300 nm wavelength range were acquired. Since CdS is a straight bad gap material, the band gap and absorption coefficient are connected by

$$\alpha \propto (h\nu - E_g)^2 \quad (1)$$

$(\alpha h\nu)^2$ vs hν, as shown in Fig. 1, allowed for the subsequent determination of the optical band gap (E_g) for the sample. At 2.41 eV on the E_g axis, it is extrapolated [5].

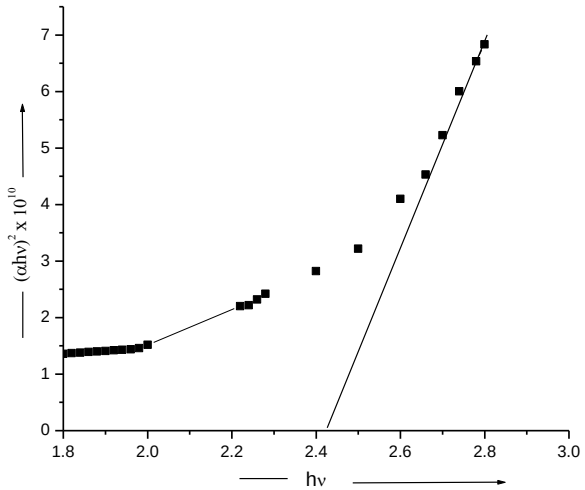

Fig. 1. A plot of $(\alpha h\nu)^2$ vs hν typical as deposited CdS thin film.

3.2. XRD Studies

The wurtzite structure of pure CdS films has been demonstrated to be hexagonal. At d values equal to 3.353 A°, 2.962 A°, 2.066 A°, and 1.765 A°, four dominating reflections correspond to the (002), (101), (110), and (112) reflections, respectively as seen in Fig. 2. This suggests that the structure of the CdS film is hexagonal wurtzite. Given that the reflected intensities (I/I_{max}) for these peaks are constant at 100 for the greatest diffraction peak (101), the reflected intensities (I/I_{max}) for these peaks are also constant [5]. It was found that the average crystallite size of the CdS film was 21.50 nm.

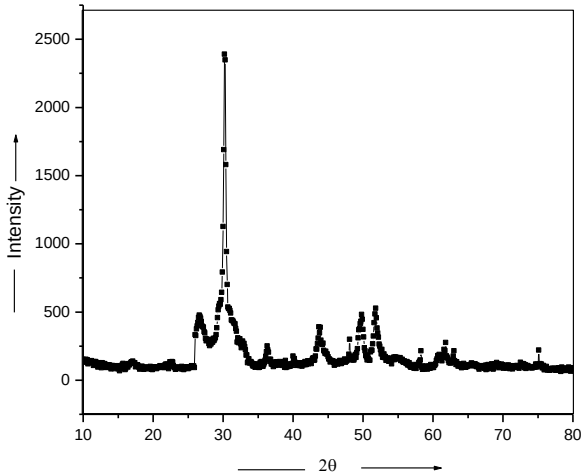

Fig. 2. XRD diffractogram of CdS thin film.

Table 1. Lattice parameters for CdS thin film.

Lattice parameters CdS (Hex)		
a (Aº)	c (Aº)	/a
4.032	6.705	.6629

3.3. The Electrical Transport Studies

3.3.1. The electrical conductivity studies

For both heating and cooling cycles, the electrical conductivities of each of these polycrystalline CdS film structures were tested in the 300–550 K temperature range. The electrical conductivity increased as the operating temperature rose, according to the tests. This demonstrates the material's semiconducting nature. The link between electrical conductivity and the CdS thin film's operating temperature is shown in Fig. 3.

It is observed that the conduction area is bifurcated. When the temperature is raised, a straight-line area with a low gradient changes to one with a larger gradient, indicating that the materials may have several conduction pathways [3, 5, 6–8]. The data might be fitted to an exponential temperature fluctuation of the conductivity in higher temperature regions.

[DOI: 10.22068/ijmse.3530]

$$\sigma_{(T)} = \sigma_{(0)} \exp(\frac{-E_{a\sigma}}{KT}) \quad (2)$$

where K is the Boltzman constant and $E_{a\sigma}$ is the conductivity activation energy. This has shown that the restricted conduction mechanism via grain boundary scattering may exist. This was verified by plotting log ($\sigma T^{1/2}$) vs 1/T, as proposed by Seto [3], Powell [9], and Oumous and Hadiri [10]. A CdS sample curve is shown in Fig. 4.

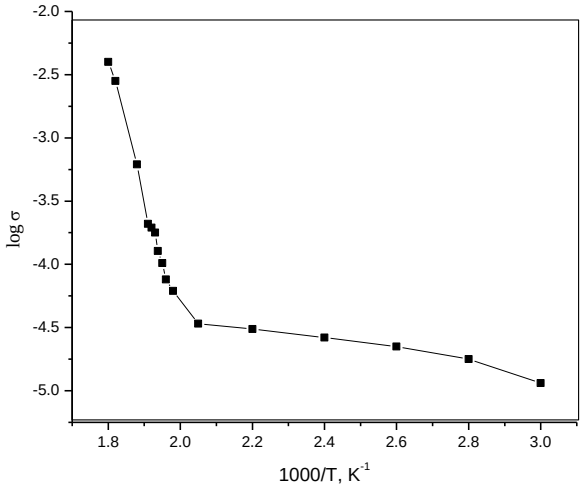

Fig. 3. Variation of electrical conductivity with working temperature for sample.

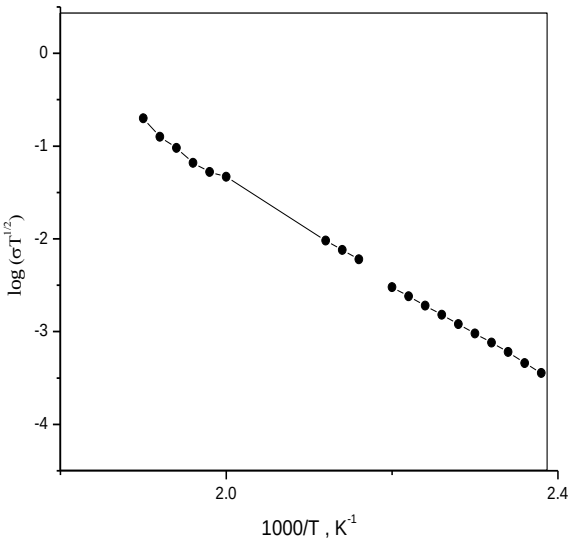

Fig. 4. Plots of log (σ $T^{1/2}$) versus 1000/T for CdS sample.

The conductivity deviates from the Arrhenius behavior at the low-temperature area, and there are very few temperature changes in conductivity. This implies that there may be variable range hopping conduction in this area due to electron tunnelling between localized states. According to Mott [11], the variable range hopping conduction is provided by;

$$\sigma = \sigma_{n0} \exp[(-T_0/T)^{1/4}] \quad (3)$$

where,

$$\sigma_{n0} = (3e^2\nu_{ph})/(8\ \pi\ K)^{1/2}[N(E_F)/\propto T]^{1/2} \quad (4)$$

$$T_0 = (\lambda \propto^3)/[KN(E_F)] \quad (5)$$

where N (E_F) is the localized state density for electrons at the Fermi level, $\propto$ is the inverse localization length of the wave function for the localized state, is a dimensionless constant, and ν_{ph} is the photon frequency at the Debye temperature. The relation may be obtained from equations (3), (4), and (5).

$$\log\left(\sigma T^{\frac{1}{2}}\right) \alpha T^{1/4} \quad (6)$$

can be inferred. Thus we have applied equation (6) to our experimental observations, which are plotted as log ($\sigma T^{1/2}$) vs $T^{-1/4}$ as shown in Fig. 5.

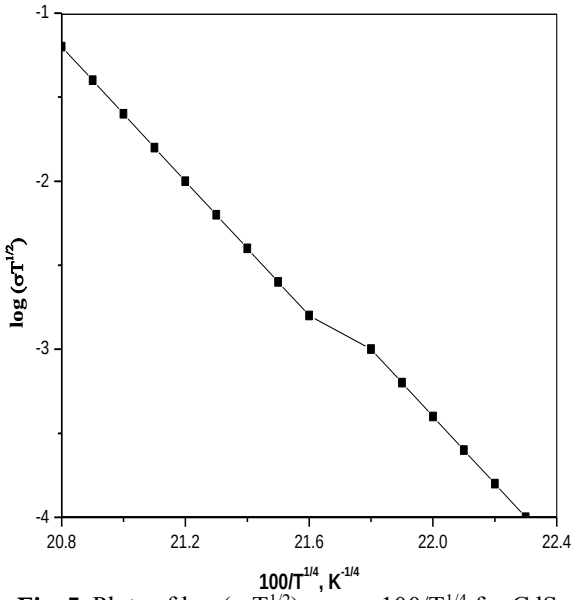

Fig. 5. Plots of log (σ $T^{1/2}$) versus $100/T^{1/4}$ for CdS sample.

The charts are linear suggesting that equation (6) holds valid in the low-temperature zone. This has indicated that the major mechanism in the low-temperature region is the variable range hopping conduction mechanism [3, 7, 6-12]. The flaws linked to the polycrystalline thin films directly result in the localized states that drive this conduction process [13-15]. These flaws might most likely be caused by partial atomic bonding at grain boundaries and partial stoichiometric departure in our samples. Next, the activation energies for both high and low temperatures were

[DOI: 10.22068/ijmse.3530]

calculated for both high and low-temperature regions and are tabulated in Table 2. The donor levels are produced below the bottom of the conduction band with $E_d = 2E_{a\sigma}$. The E_d's are listed in Table 2.

3.3.2. *The research into thermoelectric power*

Thus, the temperature range of 300 K to 550 K was used to record the TEP for the CdS thin film. The samples exhibited conduction of the n-type. For CdS samples, the temperature dependency of TEP (P) is shown in Fig. 6.

It is evident that the thermoelectric power rose as the temperature rose, and this behavior supports the theory that electrons play a key role in electrical conductivity.

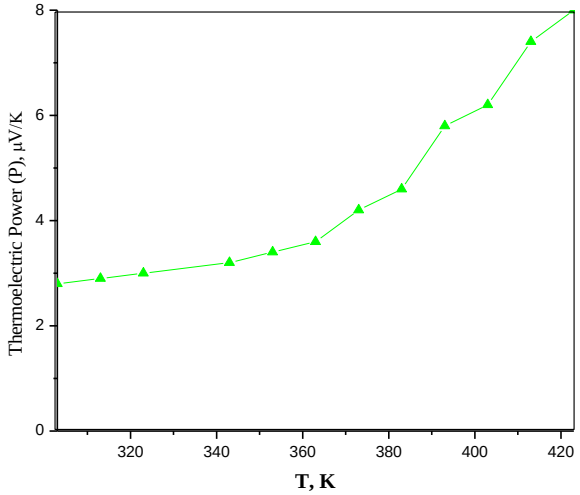

Fig. 6. Variation in thermoelectric power with the working temperature for CdS.

The thermoelectric power's temperature dependence is quasilinear, indicating the sample's degeneracy [6, 7, 18-19]. The following relationship between the thermopower and the applied temperature has been fitted to our data [6, 18, 19].

$$P = (-K/e)[A + \ln \{2(2\pi m_d^* KT)^{3/2}/nh^3\}] \quad (7)$$

where the other words have their customary meaning and A is a thermoelectric component that is dependent on the different scattering processes. For the values of n, equation (7) may be solved and rearranged, and the temperature dependence of the carrier concentration is then;

$$\log n = 3/2 \log T - 0.005P + 15.7198 \quad (8)$$

Equation (8) was then utilized to obtain the carrier densities for the CdS sample at different working temperatures. The conventional relation was then used to get the carrier mobilities (μ).

$$\mu = \sigma / ne \quad (9)$$

where the electronic charge is denoted by e, the carrier concentration by n, and the electrical conductivity by σ. Using Petritz's grain boundary scattering model, the temperature dependence of the carrier mobility was then examined to determine the inter-grain barrier potential [4, 19, 20]. Petritz states that the mobility depending on grain boundary scattering is given by;

$$\mu = \mu_0 \exp(-\phi_B/KT) \quad (10)$$

where ϕ_B is the intercrystalline barrier height and μ_0 is a pre-exponential factor based on the idea that current passes across the barrier by thermionic emission. Thus, a straight line should result from plotting log ($\mu T^{1/2}$) vs 1/T. The presence of the grain boundary scattering mechanism is demonstrated by the linear plots of log ($\mu T^{1/2}$) versus 1/T for the CdS sample, as shown in Fig. 7 [6, 7, 20]. Next, using the slopes of straight lines, the intercrystalline barrier potentials (ϕ_B) for these films were computed and are listed in Table 2.

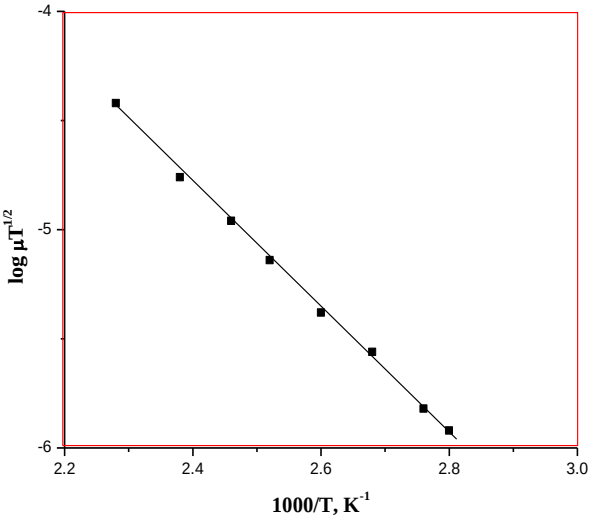

Fig. 7. The plots of log ($\mu T^{1/2}$) vs 1/T for CdS thin film.

Table 2. Some characteristics of the CdS thin film.

CdS Thin Film	Eg (eV)	Power factor (m)	Eaσ, (eV)		Ed, (eV)	Barrier Potential (ϕ_B) (eV)
			H.T	L.T		
	2.42	0.49	1.197	0.567	1.134	

[DOI: 10.22068/ijmse.3530]

4. CONCLUSIONS

The CdS thin film was found to have a polycrystalline hexagonal structure with a strong (101) preferred orientation, according to XRD tests. The E_g optical bandgap is 2.41 eV, and the CdS thin film has a high absorptivity (=10^4-$10^5 cm^{-1}$). According to electrical conductivity research, low-temperature electrical conduction is of the variable range hopping type, whereas high-temperature electrical conductivity is controlled by a grain boundary scattering restricted conduction mechanism. The operating temperature and the composition of the film have an impact on the carrier concentration and mobility.

ACKNOWLEDGEMENTS

The authors would like to thank Professor J. B. Yadav, I/c Head, USIC-CFC for providing XRD. I am also grateful to Principal Dr. Madhav Bapat, D.B.J. College, Chiplun for his encouragement and moral support in pursuing my research work.

REFERENCES

[1]. K. L. Chopra and S. R. Das., in "Thin Film Solar Cells", (eds) K L Chopra and S. R. Das, Plemun Press, New York, 1983, USA.

[2]. E. Shanthi, A. Banerjee, V. Dutta and K.L. Chopra, "Electrical and optical properties of tin oxide films doped with F and (Sb+ F)" J. Appl. Phys. 1982, 53, 1615.

[3]. L. P. Deshmukh, Ph.D. Thesis, Shivaji University, Kolhapur, M. S. 1985, India.

[4]. G. S. Shahane, Ph. D. Thesis, Shivaji University, Kolhapur, M. S. 1997, India.

[5]. Mane S.T., Lendave S.A., Pingale P.C., Suryawanshi R.V., Karande V.S., Pirgonde B. R. and Deshmukh L.P., Proc. International Conference On Advanced Materials and Nanoparticles, Oct 21-23, 2011, Kathmandu, Nepal.

[6]. S. A. Lendave, V. S. Karande and L. P. Deshmukh, "Crystallographic and microscopic investigations on chemically synthesized mercury cadmium sulphide (mcs) thin composite films", J. Surf. Engg. & Appl. Electrochem. 2010, 46, 462.

[7]. S. A. Lendave, V. S. Karande and L. P. Deshmukh, "Structural and transport characteristics of HgxCd1-xS thin composite films: A correlation" J. Metallurgy & Mat. Sci. 2010, 52, 363.

[8]. J. C. Manifacier. L. Szepessy, J. F. Bresse, M. Perotin and R. Struck, "In_2O_3:(Sn) and SnO_2:(F) films—Application to solar energy conversion; part 1—Preparation and characterization" Mater. Res. Bull. 1979, 14, 109.

[9]. P. D. More, G. S. Shahane, P. N. Bosale, A. A. Belhekar, M. K. Dongare and L. P. Deshmukh, "Micro-crystallographic and spectral response studies of $CdSe_{1-x}$ Te_x alloyed thin films" Ind. J. Pure & Appl. Phys. 2002, 40, 62.

[10]. M. M. Abou Sekkina, A. Tawfik and M.I. Abd El-Ali, "Further studies on the temperature dependence of the electric and photovoltaic properties of CdSe thin films for solar cells" Thermochimica Acta 1985, 86, 59.

[11]. Y. D. Tembhurkar and J. P. Hirde, "Structural, optical and electrical properties of spray pyrolytically deposited films of copper indium diselenide" Thin Solid Films 1992, 215, 65.

[12]. J. W. Orton and M. J. Powell, "The Hall effect in polycrystalline and powdered semiconductors", Rep. Progr. Phys. 1980, 43, 1263.

[13]. Oumous and H. Hadiri, "Optical and electrical properties of annealed CdS thin films obtained from a chemical solution" Thin Solid Films 2001, 386, 87.

[14]. N. F. Mott, Phil., Mag. 1969, 19, 835.

[15]. L. I. Soliman, "Influence of γ-irradiation on optical and electrical properties of amorphous CuInSeTe, CuInSTe and CuInSeS thin films", Ind. J. Pure & Appl. Phys. 1994, 32, 166.

[16]. T. Suzuki, Y. Ema and H. Toshiya, "In doping in CdTe film by co-evaporation of CdTe and In" Jpn. J. Appl. Phys. 1987, 26, 2009.

[17]. V. B. Pujari, S. H. Mane, V. S. Karande and L. P. Deshmukh, „ A study of cadmium mercury telluride (CMT) thin film structures: some physical observations and characteristics", Mat. Chem. Phys. 2004, 83, 10.

[18]. V. B. Pujari, D. J. Dhage and L. P. Deshmukh, "n-$HgxCd_{1-x}Se$ thin film electrodes for photoelectrochemical

[DOI: 10.22068/ijmse.3530]

applications", Ind. J. Engin. & Mat. Sci, 2008, 15, 275.
[19]. L. P. Deshmukh, S. G. Holikatti and B. M. More, "Optical and structural properties of antimony-doped CdS thin films", Mat. Chem. Phys. 1995, 39, 278.
[20]. Deshmukh LP, Rotti CB, Garadkar KM, Shahane GS. "Structural and electrical properties of indium doped Cdo. 7. Zno. 3S thin", Ind. J. Pure & Appl. Phys. 1998, 36, 322.

[DOI: 10.22068/ijmse.3530]